

## OBSERVATIONS OF A SERIES OF SIX RECENT GLITCHES IN THE CRAB PULSAR

TONY WONG AND D. C. BACKER

Astronomy Department and Radio Astronomy Laboratory, University of California, Berkeley, CA 94720

AND

A. G. LYNE

University of Manchester, Jodrell Bank Observatory, Macclesfield, Cheshire, SK11 9DL, United Kingdom

*To appear in the Astrophysical Journal*

### ABSTRACT

From 1995 to 1999, daily monitoring of the radio emission from the Crab pulsar at the Green Bank and Jodrell Bank observatories revealed a series of six sudden rotational spinups or glitches, doubling the number of glitches observed for this pulsar since 1969. With these observations, the range of time intervals between significant Crab glitches has widened considerably, indicating that the occurrence of Crab glitches may be more random than previously thought. The new glitch amplitudes  $\Delta\nu/\nu$  span an order of magnitude from  $2 \times 10^{-9}$  to  $3 \times 10^{-8}$ . Except in one case, which we suggest may represent an “aftershock” event, the frequency jumps display an exponential recovery with a timescale of  $\sim 3$  days for the smaller glitches and  $\sim 10$  days for the largest (1996) glitch. In the largest event, a portion of the spinup was resolved in time, as was previously reported for the 1989 glitch. A pronounced change in  $\dot{\nu}$  also occurs after each glitch and is correlated with the size of the initial frequency jump, although for some of the smaller glitches this appears to be a temporary effect. We discuss the properties of the ensemble of observed Crab glitches and compare them with the properties of Vela glitches, highlighting those differences which must be explained by evolutionary models.

*Subject headings:* pulsars: individual (Crab) — stars: neutron

### 1. INTRODUCTION

Pulsar timing observations reveal that sudden increases in rotation rate, known as *glitches*, are a common feature in some pulsars, especially younger ones (Shemar & Lyne 1996). These spinup events are superposed on the long-term rotational slowdown of the pulsar due to magnetic dipole radiation and particle outflow, and are usually followed by a relaxation towards the extrapolated pre-glitch frequency over a period of days to weeks. Continuous monitoring of the Crab pulsar (PSR B0531+21) uncovered six significant glitches from 1969 to 1992, at intervals of 3–6 years (Lyne, Pritchard, & Smith 1993). High glitch activity has been observed in other pulsars as well. For example, at least twelve glitches of the Vela pulsar (PSR B0833–45) were observed between 1969 and 1996 (e.g., Chau et al. 1993; Flanagan 1995), usually at intervals of 2–3 years, and twelve glitches have been detected in the rotation of PSR J1341–6220 during just 8.2 years of observations (Wang et al. 2000), making it the most frequently glitching pulsar known.

At the same time, precise timing measurements have revealed that many pulsars exhibit an unpredictable fluctuation in pulse arrival time known as *timing noise*. A number of previous studies (Boynton et al. 1972; Groth 1975; Cordes 1980) have shown that timing noise in the Crab pulsar can be modeled as a random walk in frequency. The individual steps in this random walk have not been resolved, but can be of either sign and have amplitudes  $|\Delta\nu/\nu| \ll 10^{-10}$ , whereas major glitches of the Crab can be distinguished as sudden positive jumps in frequency with  $\Delta\nu/\nu \gtrsim 10^{-9}$ , followed by an exponential recovery over a period of days to months. Still, the possibility re-

mains that glitches lie at the upper end of a continuous spectrum of frequency jumps (Cordes & Helfand 1980), and careful consideration of observational selection effects is essential before attempting to draw general conclusions about glitches.

Although our understanding of the glitch phenomenon is limited by our incomplete knowledge of neutron star structure, the most plausible explanation for the frequency spinups is the dumping of angular momentum from an unseen reservoir into the part of the star whose rotation we measure (e.g., Alpar et al. 1993). Since the outer crust and core superfluid are believed to be coupled on short ( $< 1$  minute) timescales to the magnetic field and the observed pulsar beam (e.g., Alpar, Langer, & Sauls 1984; Mendell 1998), the probable site of this reservoir is a superfluid component in the inner crust. As discussed by Anderson & Itoh (1975) and others, the quantized vortex lines which carry angular momentum in the superfluid can be “pinned” to lattice sites in the neutron-rich inner crust, inhibiting the outward motion of vortex lines that occurs as the star spins down and creating an excess rotation of the superfluid relative to the outer crust. If large numbers of pinned vortices were to simultaneously unpin, the excess angular momentum would be shared with the rest of the star and a glitch would be observed. While this scenario provides an attractive theoretical framework for understanding glitches, the mechanisms that trigger glitches and lead to the observed postglitch recovery remain controversial (e.g., Alpar et al. 1996; Link & Epstein 1996; Jones 1998).

Observations of pulsar glitches, in addition to providing insights into the glitch phenomenon itself, offer one

of the few direct probes of neutron star structure and the physics of ultradense matter. For instance, the frequent large glitches ( $\Delta\nu/\nu \sim 10^{-6}$ ) seen in the Vela pulsar indicate that the superfluid component in the inner crust comprises  $\sim 2\%$  of the star’s moment of inertia (e.g., Chau et al. 1993; Link, Epstein, & Lattimer 1999). Crab glitches, on the other hand, exhibit much smaller relative frequency jumps ( $\Delta\nu/\nu \sim 10^{-8}$ ), and tend to be dominated by persistent changes in the slowdown rate with  $\Delta\dot{\nu}/\dot{\nu} \sim 10^{-4}$  (e.g., Gullahorn et al. 1977; Demiański & Prószyński 1983). The persistent shift in  $\dot{\nu}$  has been attributed to either a change in the external torque (Link, Epstein, & Baym 1992) or a change in the moment of inertia acted on by the torque (Alpar et al. 1996). The various exponential relaxation timescales that follow glitches have been interpreted, in the framework of the “vortex creep” theory, as resulting from distinct regimes of superfluid pinning to the crustal lattice (Alpar et al. 1993).

Since the occurrence of glitches is unpredictable and their relaxation timescales can be quite short (a few days or less), daily monitoring of frequent glitchers such as the Crab and Vela pulsars are necessary in order to study the glitch process in detail. Here we present radio timing observations taken during a period of increased glitching in the Crab that began in 1995 and has extended into 2000. The data were collected as part of regular pulsar monitoring programs with dedicated small telescopes at the NRAO<sup>1</sup> Green Bank and the University of Manchester Jodrell Bank sites. The data acquisition and reduction procedures are described in §2, and in §3 we present our analysis of six distinct frequency jumps during this period. A large glitch was observed in 1996 June and smaller events were observed in 1995 October, 1997 January, February, and December, and 1999 October. (The recent large glitch on 2000 July 15 is not covered by these observations). In §4 we examine the frequency (rate of occurrence) of Crab glitches, and §5 we discuss the observed properties of the glitches. Our conclusions are summarized in §6. Throughout this paper we define the rotation frequency  $\nu$  in Hz, which can be converted to angular frequency using  $\Omega=2\pi\nu$ .

## 2. OBSERVATIONS AND DATA REDUCTION

Observations at the Green Bank (hereafter GB) site of the NRAO are conducted as part of a regular monitoring program on a 26 m (85 ft) radio telescope. The Crab pulsar is observed daily, with typically eight 10-minute integrations at 610 MHz and three integrations at 327 MHz. Two linear polarizations are measured separately and combined later in the data analysis software. A convolution processor dedisperses the signal in real time within each of 32 frequency channels of 0.5 (0.25) MHz bandwidth at 610 (327) MHz, thus correcting for pulse smearing across each channel due to interstellar dispersion. The signal is then averaged synchronously with the predicted apparent pulse period into approximately 1000 time bins (1 bin  $\approx 34 \mu\text{s}$ ). A time stamp accurate to  $\sim 0.1 \mu\text{s}$  is recorded at the start of each integration. For calibration purposes, integrations on a standard noise source are performed before the source integrations.

<sup>1</sup>The National Radio Astronomy Observatory (NRAO) is operated by Associated Universities, Inc, with funding from the National Science Foundation.

In software, the integrated profiles from all 32 channels are aligned using the assumed dispersion measure (DM), flux calibrated, and summed to form a single pulse profile for each integration. A high signal-to-noise average profile from several integrations is used as a template, and a simple cross-correlation is performed to determine the arrival time (TOA) of the main pulse peak. A mean TOA for each day or half-day is then determined using a least-squares linear fit to all of the TOA’s during that period, as in Shemar & Lyne (1996). An associated uncertainty is also derived from this least-squares fit. The typical uncertainty in the day-averaged TOA at 610 MHz is  $10 \mu\text{s}$ , but increases to around  $60 \mu\text{s}$  during periods of heightened interstellar scattering, as indicated by broadening of the 327 MHz pulse profiles (see below). Arrival times are then corrected to the solar system barycenter using the standard TEMPO software package (Taylor & Weisberg 1989).

Observations at the University of Manchester’s Jodrell Bank Observatory (hereafter JB) are conducted at 610 MHz with a 12.5-m telescope as part of a long-term program of monitoring the Crab pulsar. The pulsar is observed daily over a timespan of up to 14 hours; a full description of the data acquisition and reduction techniques can be found in Lyne et al. (1993). The 610-MHz data are supplemented by occasional observations at 1400 MHz using the 76-m Lovell telescope, in order to monitor changes in DM. Because the on-source integration times with the 12.5-m telescope are much longer than for the GB observations, the uncertainties in the day-averaged TOA’s are comparable to those for the GB data ( $\sim 10 \mu\text{s}$ ). There are, however, variations of up to  $\sim 50 \mu\text{s}$  in the offset between the two datasets during periods of increased scattering, probably a result of changes in the observed pulse profile. Thus when combining the datasets, we restricted ourselves to periods of minimal scattering during which the offset was roughly constant.

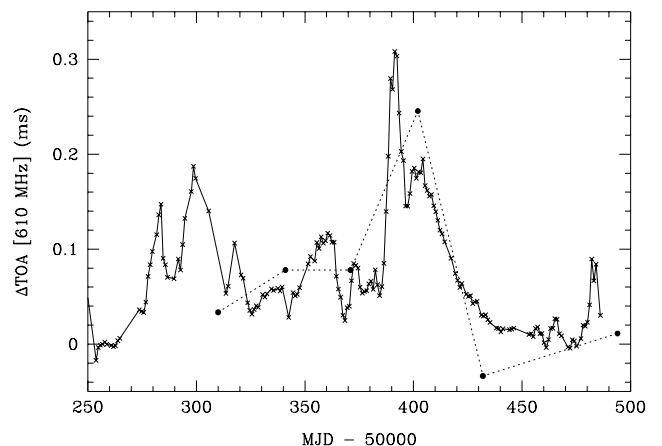


FIG. 1.— Estimated TOA fluctuations at 610 MHz due to changes in dispersion measure (DM). The DM fluctuations are determined by comparison of the 610 MHz and 327 MHz pulse arrival times, after the 327 MHz data have been corrected for scattering (see text). Since we have not determined absolute arrival times, the zero point of the y-axis is defined as MJD 50259. The filled circles are points from the Jodrell Bank DM monitoring programme, with a reference DM of 56.82 chosen to produce a rough match with the GB data.

In this paper we confine our analysis to the 610 MHz data, principally from Green Bank but with the JB data included during periods of sparse sampling. The 327 MHz GB data proved to be of lower quality for timing purposes, but were useful for monitoring changes in scattering and dispersion (e.g., Backer, Wong, & Valanju 2000), which can produce systematic errors in the 610-MHz TOA's. Interstellar scattering leads to pulse broadening due to multipath propagation, which can be modeled by assuming that the intrinsic pulse shapes are Gaussian and convolving the profile with a one-sided exponential decay (e.g., Komesaroff, Hamilton, & Ables 1972). Variable scattering was found to be important at 327 MHz but generally not at 610 MHz, due to its strong frequency dependence. Changes in DM were monitored by correcting the 327 MHz data for scattering using the exponential model, then taking the difference of the 610 MHz and 327 MHz timing residuals with a common spindown model applied to both data sets. From these measurements we inferred that DM changes can contribute offsets of up to  $\sim 100 \mu\text{s}$  to the 610 MHz TOA's, although the changes generally occur gradually over several weeks (Figure 1). As an example, a DM change of  $10 \mu\text{s}$  per day leads to an error in the rotation frequency of  $\sim 5 \times 10^{-9}$  Hz, which is at least an order of magnitude smaller than the glitch events described here. In light of the uncertainties in the scattering correction and a lack of daily DM measurements during some epochs, we have generally chosen not to apply a DM correction to our timing data. However, in the months following 1997 October ( $\sim$  MJD 50723) the DM was found to change extremely rapidly (§3.4), and for Glitch 11 (§3.5) we have attempted to include these effects in our modeling.

### 3. RESULTS OF GLITCH MODEL FITTING

For the study of both glitches and timing noise, one commonly fits to the arrival-time data (expressible as rotational phase  $\phi$ ) a simple spindown model of the form:

$$\phi_m(t) = \phi_0 + \nu_0(t - t_0) + \frac{1}{2}\dot{\nu}_0(t - t_0)^2 + \frac{1}{6}\ddot{\nu}_0(t - t_0)^3, \quad (1)$$

where  $\phi_m(t)$  is the predicted pulse phase at time  $t$  and  $t_0$  is an arbitrary reference time. Timing irregularities appear as *phase residuals* ( $\phi - \phi_m$ ), deviations of the observed pulse phase from the predicted phase. *Frequency residuals* ( $\nu - \nu_m = \dot{\phi} - \dot{\phi}_m$ ) are then calculated by averaging the phase residuals over  $\sim 1$  day intervals and determining the slope between adjacent points. We estimate that the typical error in the frequency determinations is  $5 \times 10^{-9}$  Hz except during periods of severe scattering. In Figure 2 (upper panel) the frequency residuals from the GB data are shown, based on a model fitted to the JB data over the 500 days prior to the 1996 glitch. The values of  $\nu$ ,  $\dot{\nu}$ , and  $\ddot{\nu}$  just before this glitch, as determined by the model, are given in Table 1. In the lower panel of Fig. 2 a quadratic fit to the residuals following this glitch (corresponding to jumps in  $\nu$ ,  $\dot{\nu}$ , and  $\ddot{\nu}$ ) has been removed to permit closer inspection of the residuals.

After subtracting a preglitch spindown model given by Equation (1), we characterize a sudden glitch event by permanent jumps in  $\nu$ ,  $\dot{\nu}$ , and  $\ddot{\nu}$  accompanied by exponentially decaying jumps in  $\nu$ . Shemar & Lyne (1996) have applied such a model to a large sample of glitching pulsars. If  $t$  is the time since the glitch, then the postglitch frequency

residuals can be written as:

$$\Delta\nu = \Delta\nu_p + \Delta\dot{\nu}_p t + \frac{1}{2}\Delta\ddot{\nu}_p t^2 + \sum_n \Delta\nu_n e^{-t/\tau_n}. \quad (2)$$

Thus, at the glitch time ( $t = 0$ ) the initial unresolved step in frequency is given by

$$\Delta\nu_0 = \Delta\nu_p + \sum_n \Delta\nu_n. \quad (3)$$

To minimize the number of fitting variables, we have assumed that all postglitch components begin simultaneously (at  $t = 0$ ).

In order to take advantage of all available data, the glitch model was rewritten in terms of rotational phase and fitted directly to the TOA's that had been averaged into 0.5–1 d intervals. Results of the fitting are summarized in Table 2. For each glitch up to three models are shown, each employing a different parameter set or range of data; the maximum length of the data span is prescribed by the interval between glitches. The nonlinear least-squares fitting routine we used seeks to minimize the reduced  $\chi^2$ , defined as

$$\tilde{\chi}^2(\phi'_m) = \frac{1}{N - M} \sum_{i=1}^N \left( \frac{\phi - \phi'_m}{\sigma_i} \right)^2, \quad (4)$$

where  $N$  is the number of points in the fit,  $M$  is the number of fit parameters,  $\phi'_m$  is the model phase (including the glitch model), and  $\sigma_i$  is the uncertainty in each phase measurement (§2). Also shown in Table 2 is  $\tilde{\chi}^2(\nu'_m)$ , which describes how well the model *frequencies* fit the observed frequencies. Each transient term in the fit has been labeled with subscript 1, 2, or 3 based on whether it represents a short-term ( $\lesssim 50$  d) exponential decline ( $\Delta\nu_n > 0$ ), long-term ( $\gtrsim 50$  d) exponential rise or decline, or very short-term ( $\lesssim 1$  d) exponential rise ( $\Delta\nu_n < 0$ ), respectively.

Our adopted “best fits,” identified with asterisks in Table 2, are presented in Table 3, along with the corresponding parameters for the previously observed Crab glitches. (The individual glitches are discussed in more detail below.) Parameters of the first five glitches are taken from Lyne et al. (1993), after adjusting their fits to conform with the model given by Equation (2). Parameters for Glitch 6 have been derived from unpublished JB timing data.

The accuracy of the fit parameters is difficult to determine because there are inevitably correlations between parameters, there is no obvious time period over which to perform the fit, and the fit is dependent on the assumed spindown model before the glitch. Our analysis is also susceptible to systematic errors resulting from DM variations (§2), and to intrinsic timing noise in the pulsar which cannot be modeled in simple terms. The latter will tend to increase the formal  $\tilde{\chi}^2$  as the timespan of the fit increases. For events prior to 1995, the uncertainties are those given by Lyne et al. (1993). For the 1995–9 events, the quoted uncertainties are determined by shifting each parameter value above and below the best-fit value until the resulting value of  $\tilde{\chi}^2(\nu'_m)$  increases by 1. This criterion corresponds to allowing a  $1\sigma$  shift in each frequency measurement away from the model. In most cases, the other parameters were allowed to vary during this process. As a consistency check we have fitted the GB and JB data separately whenever possible; error bars have been extended when necessary to encompass the resulting fits. The quoted errors do not include the uncertainty in the preglitch timing model.

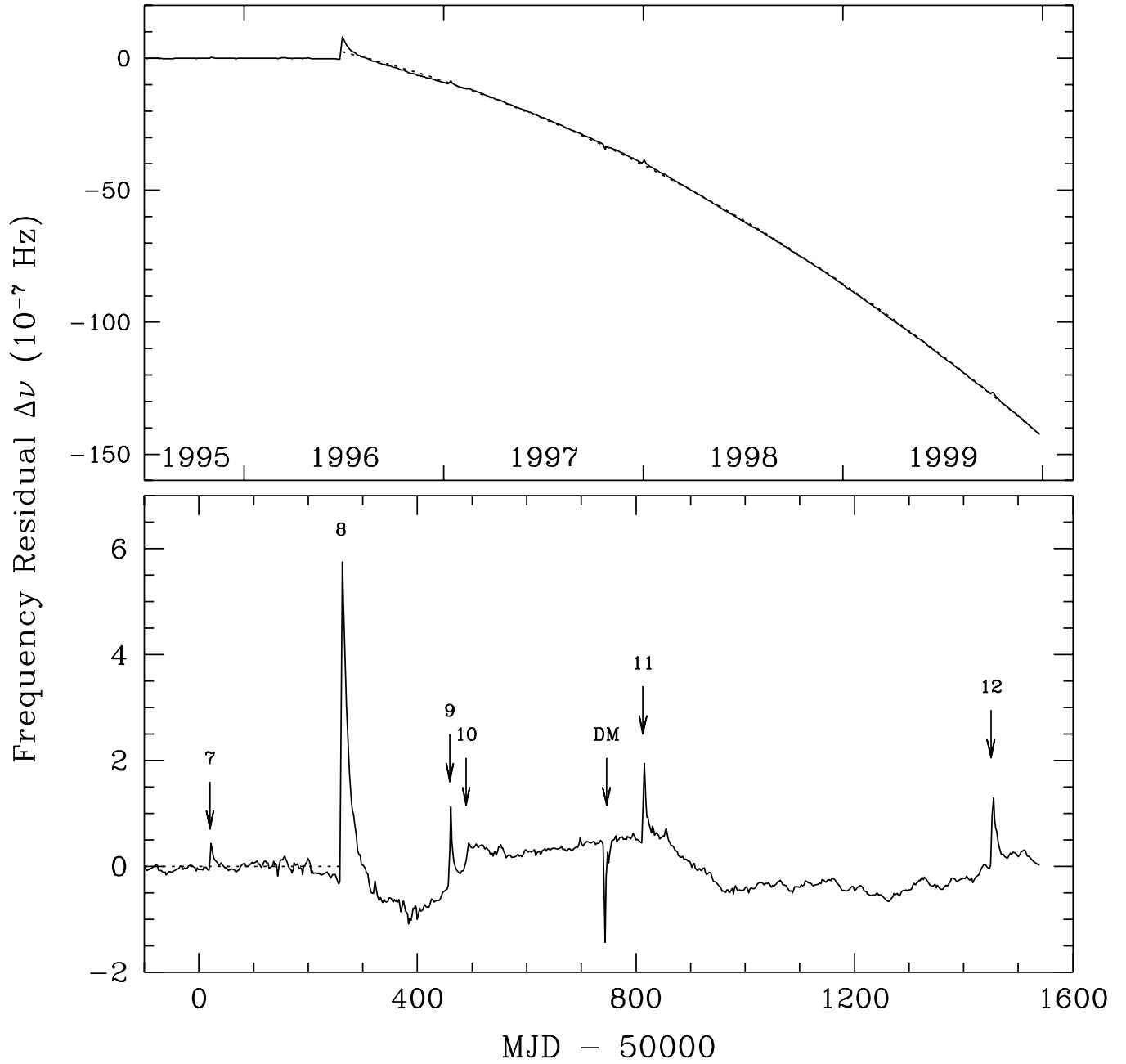


FIG. 2.— Frequency residuals derived from GB data, after subtraction of a model fit to the 500 days before the 1996 June glitch. In the bottom panel, a quadratic fit to the residuals from MJD 50350–51400 has been removed (dotted line in the top panel) in order to highlight discrete events.

### 3.1. Glitch 7: MJD 50020

This small event ( $\Delta\nu/\nu \sim 2 \times 10^{-9}$ ) is easily distinguished from the general timing noise when viewed in the frequency residuals (Fig. 2). It may be similar to the small 1971 event reported by Lohsen (1972), although in that case gaps in the timing observations make it difficult to establish whether an exponential decay was present. Due to the small size of the glitch and a systematic variation by  $\sim 10 \mu\text{s}$  in the offset between the GB and JB residuals, we have fitted a glitch model to the JB residuals only rather than attempting to combine the datasets. Fits to the GB dataset are consistent with the adopted fit within the stated errors.

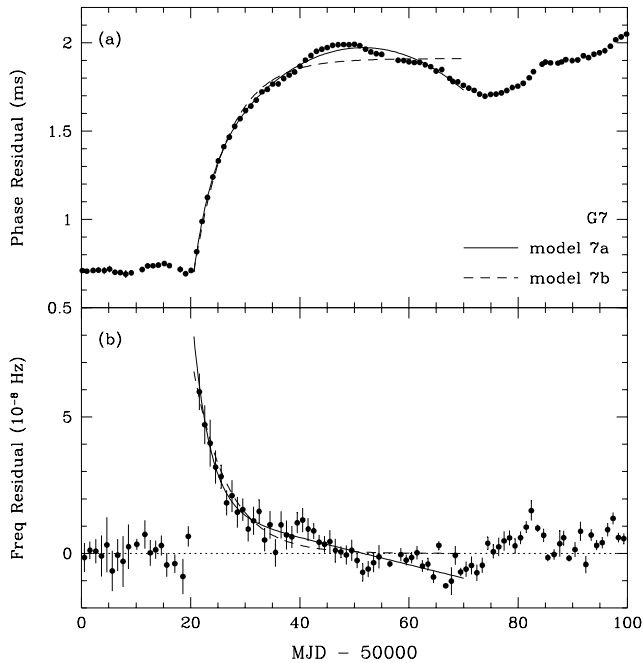


FIG. 3.— Phase and frequency residuals showing the effects of Glitch 7 in 1995 October. Two postglitch timing models are shown, one with a temporary jump in  $\dot{\nu}$  (solid line) and one with only a transient exponential term (dashed line).

Figure 3 displays the JB phase residuals in milliseconds [i.e.,  $(\phi - \phi_m)P$  with  $P = 1/\nu$ ] and the frequency residuals in units of  $10^{-8}$  Hz after removing a spindown model fitted to the 300 d prior to the event. The solid line is the adopted glitch model of the form given by Eq. (2) without the  $\Delta\ddot{\nu}$  term, fitted to the 50 days after the glitch. Note that the model includes a temporary change in  $\dot{\nu}$  over this timespan that vanishes around MJD 50075. The dashed line represents a simpler model consisting of only a pure exponential decay (no “persistent” jump in  $\nu$  or  $\dot{\nu}$ ), which is a much poorer fit to the data more than 20 d after the glitch. On the other hand, since the residuals for even this simple model are not significantly greater than the general timing noise, such a model could still be a valid description of the data.

### 3.2. Glitch 8: MJD 50260

On 1996 June 25–26, the pulsar rotation frequency experienced a large jump of  $\Delta\nu/\nu \sim 3 \times 10^{-8}$ , of which roughly 1/3 may have been resolved in time, as will be ar-

gued below. For the analysis, the preglitch timing model used in Fig. 2 was adopted, while a postglitch recovery model was fit to the following 190 days (since the recovery was interrupted by another glitch in 1997 January). The Jodrell Bank data were included only during the periods MJD 50200–50280, 50325–50375 and 50410–50450, when scattering effects were judged to have negligible impact on the offset between the two datasets. The  $1\sigma$  uncertainty in the offset is about  $15 \mu\text{s}$ .

In addition to permanent jumps in  $\nu$  and  $\dot{\nu}$  and an exponential decay with a timescale of  $\tau_1 \sim 10$  d, there is a long-term component that can be modeled either as an exponential decay with a timescale of  $\tau_2 \sim 100$  d, or as a “permanent” (up to the next glitch) positive jump in  $\ddot{\nu}$ . As noted by Shemar & Lyne (1996), this ambiguity results from the fact that the exponential time constant  $\tau_2$  is comparable to the timespan of the fit. While the model with a change in  $\ddot{\nu}$  provides a better fit to the data ( $\tilde{\chi}^2$  of 831 rather than 911), in both cases  $\tilde{\chi}^2$  is likely dominated by unmodeled timing noise, so it is unclear whether the difference between the two is significant. (For comparison, fitting a spindown model to an equivalent interval well separated from glitches, from MJD 51000 to 51190, gives  $\tilde{\chi}^2$  of 800). In Table 2 we give the best-fit values corresponding to each of the two models (8a and 8b). The 100-d exponential decay has a timescale comparable to that observed in the 1975 and 1989 glitches (Lyne et al. 1993), but its amplitude has the opposite sign (i.e. it represents a slowdown rather than a spinup).

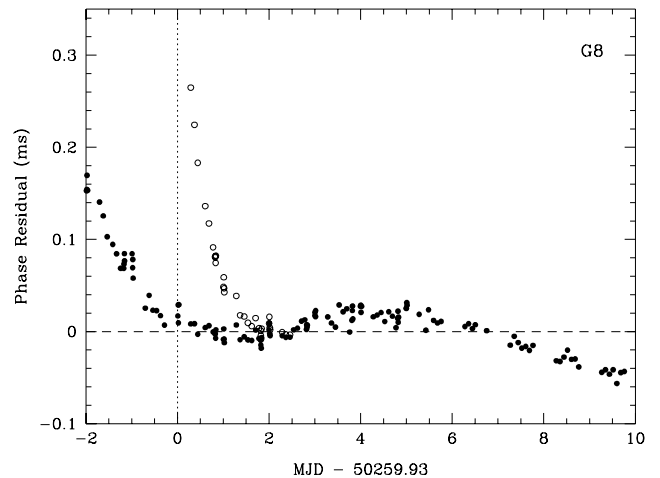


FIG. 4.— Phase residuals immediately after the 1996 glitch (G8), after removal of persistent changes in  $\nu$ ,  $\dot{\nu}$ , and  $\ddot{\nu}$ , a 10.3 d exponential decay, and a 0.5 d exponential rise. The open circles are the phase residuals if the 0.5 d rise is *not* included. The time axis is referenced to the assumed glitch time.

Upon removing the components discussed above, it becomes clear from the phase residuals that a short-term spinup of the pulsar occurred in the first two days (Figure 4). Although the magnitude of the residuals is consistent with timing noise alone, their temporal dependence (with a sudden rise and exponential-like decay) leaves little doubt that they are associated with the glitch. The fitted exponential timescale for the spinup is roughly 0.5 d and its amplitude is about  $0.5 \Delta\nu_1$ . These values are given in Table 2 as Model 8c. In comparison, the spinup time

seen in the 1989 glitch was 0.8 d and its relative amplitude was about  $0.3 \Delta\nu_1$  (Lyne, Smith, & Pritchard 1992). As was the case in 1989, part of the spinup is still unresolved ( $\Delta\nu_0 > 0$ ).

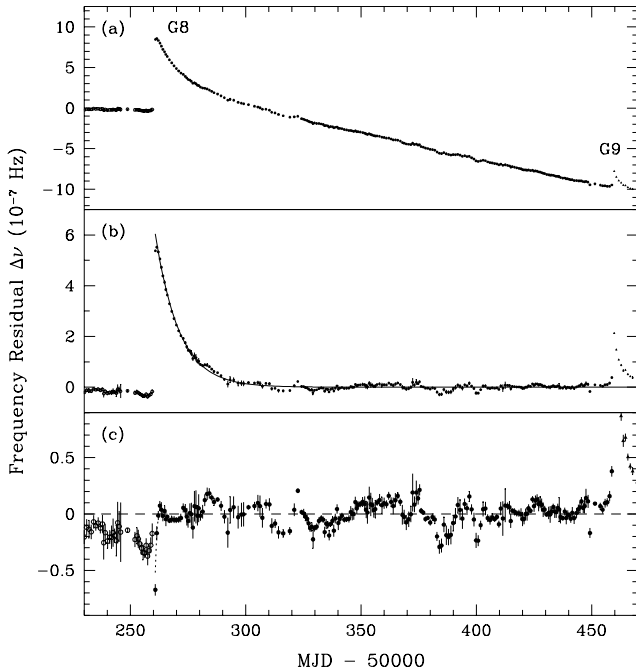


FIG. 5.— Frequency residuals around the time of the large glitch of 1996 June (G8), after (a) subtraction of only the preglitch spindown model; (b) removal of persistent changes in  $\nu$ ,  $\dot{\nu}$ , and  $\ddot{\nu}$  (the 10-d transient is shown as a solid line); (c) removal of the 10-day transient component as well (the 0.5-d transient is shown as a dotted line). Open circles are preglitch points, solid triangles are points after the 1997 January glitch (G9), and solid circles are points between the two glitches.

Figure 5 provides a visual breakdown of the components in the adopted glitch model, in which we parametrize the long-term postglitch behavior using a change in  $\ddot{\nu}$ . We begin with the frequency residuals after subtraction of the preglitch model [Fig. 5(a)]. Note that after  $\sim 50$  d the dominant effect of the glitch is a permanent increase in the spindown rate  $|\dot{\nu}|$ , as was seen in the large glitches of 1975 and 1989. In Fig. 5(b), the fitted  $\Delta\nu_p$ ,  $\Delta\dot{\nu}_p$  and  $\Delta\ddot{\nu}_p$  after the glitch have been removed. The solid line represents the fitted  $\tau_1 = 10$  d exponential. In Fig. 5(c) the 10 d transient component has also been removed, revealing the short-term rise following the glitch. Note the striking slowdown in frequency by  $\sim 3 \times 10^{-8}$  Hz that precedes the glitch, a  $5\sigma$  offset from the preglitch model. Since this slowdown takes place over a much shorter timescale ( $\sim 20$  d) than the timescale over which the preglitch model fit can vary ( $\sim 250$  d), it appears to be significant. However, as such a glitch “precursor” is not observed before the subsequent glitch 200 days later, it does not appear to be a general feature of Crab glitches.

### 3.3. Glitches 9 and 10: MJD 50459 and 50489

In early 1997, two glitches occurred roughly 30 d apart (Figure 6). The first event ( $\Delta\nu/\nu \sim 8 \times 10^{-9}$ ) occurred on MJD 50459 (1997 January 11), and was well sampled

in time, occurring within  $\sim 1$  hr of observations at GB. It is dominated by a transient term with a timescale  $\tau \approx 3$  d and shows no evidence for a resolved spinup. Although there is a measurable change in  $\dot{\nu}$ , little can be said about any change in  $\ddot{\nu}$  because the fit was performed over just 30 days. The second event ( $\Delta\nu/\nu \sim 2 \times 10^{-9}$ ), which occurred in early February during a gap in the GB observations, can be modeled as step changes in  $\nu$ ,  $\dot{\nu}$ , and  $\ddot{\nu}$  based on the GB data alone (Model 10a in Table 2); inclusion of JB data recorded during the gap indicates a gradual spinup with a timescale of  $\sim 2$  d (Model 10b, the adopted fit). Modeling the long-term recovery with an asymptotic exponential yields a much poorer fit (Model 10c). This model is also poorly constrained because  $\tau$  is much longer than the timespan of the fit, which extends up to the next glitch (MJD 50812) but excludes a period from MJD 50742-50752 as described below (§3.4).

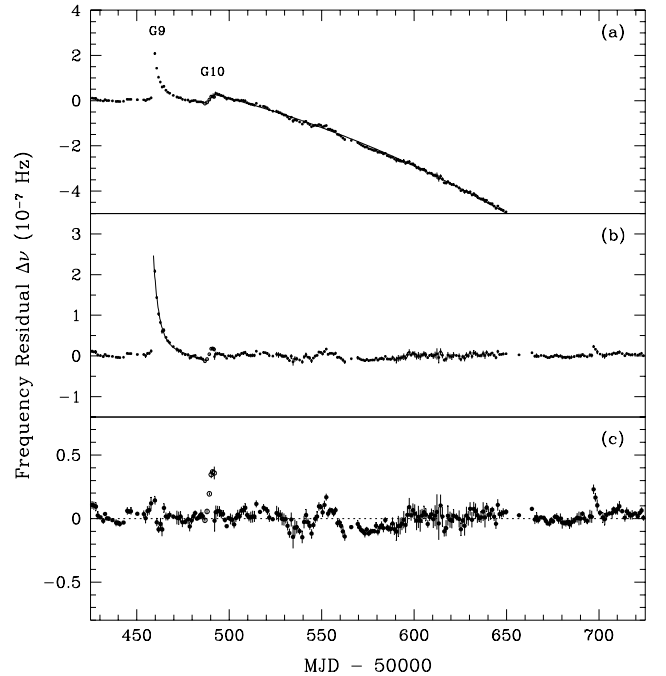


FIG. 6.— Frequency residuals before and after the early 1997 glitches (G9 and G10), after subtraction of (a) only the preglitch spindown model; (b) a model for the February event without a short-term component (Model 10a); (c) the adopted model for the January event as well (solid line in panel b). The open circles are JB data that reveal the gradual spinup associated with Glitch 10.

In some respects the February event resembles the glitches with gradual spinups observed in 1989 and 1996, yet it lacks the exponentially decaying term ( $\Delta\nu_1$ ) that dominates in all other glitches. Its close proximity in time to the January glitch is also unusual, and in §4.2 we raise the possibility that Glitch 10 is an unusually strong example of an “aftershock” phenomenon that may have been seen, to a much smaller degree, following other glitches as well. Although we refer to this event as a glitch, it quite possibly represents a different type of timing irregularity (see Wang et al. 2000, for a possible analogue in PSR J1614-5047).

One difficulty with modeling this pair of glitches is that they occur just 200 d after the preceding glitch, which

leaves only a  $\sim 100$  d timespan over which to fit a preglitch model for Glitch 9 if one wishes to safely exclude transient effects of Glitch 8. To better reflect the cumulative effects of the series of glitches, we instead used the spindown model that was fit to the 500 d prior to Glitch 8 and adjusted its values of  $\dot{\nu}$  and  $\ddot{\nu}$  by the values of  $\Delta\dot{\nu}_p$  and  $\Delta\ddot{\nu}_p$  derived for that glitch. This was then used as the preglitch model for Glitch 9, and a similar procedure was used to create a preglitch model for Glitch 10. The effects of Glitch 9 are therefore given with respect to Glitch 8, and Glitch 10 with respect to Glitch 9.

### 3.4. DM Jump around MJD 50740

In the middle of 1997 October there was a major disruption of the Crab pulsar signal which appears to be related to interstellar propagation. The event was characterized by a sharp decrease in flux as well as a noticeable jump in the pulse phase. For approximately a week (October 18–25), the 327 MHz GB data showed a second pulse profile superposed on the original one and phase shifted by  $\sim 0.2$  period (6.5 ms); subsequently the “new” profile became dominant and the “old” profile faded. A corresponding phase shift by  $\sim 0.08$  period (2.5 ms) was seen in the 610 MHz data, although the pulse signal was very weak during this interval.

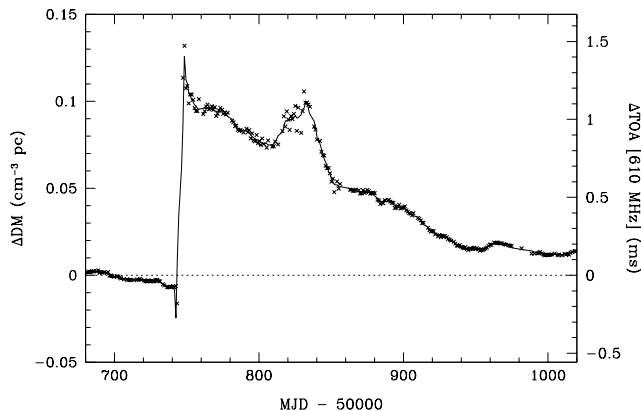


FIG. 7.— DM jump of 1997 October as measured using the 610 MHz GB data and the scattering-corrected 327 MHz GB data. The scale on the right-hand side indicates the expected change in the 610 MHz TOA’s resulting from the DM jump (compare with Figure 1). The solid line, a running 5-day boxcar smooth, is the correction applied to the 610 MHz data for Glitch 11.

The frequency dependence of the shift points to a jump in the dispersion measure of  $\approx 0.15$  pc cm $^{-3}$ , which can account for about 5.8 ms of the shift at 327 MHz and 1.6 ms at 610 MHz. The DM jump was followed by a nearly linear recovery towards the original DM (Figure 7). The remaining phase shift appears to have been non-dispersive in nature. Since both “old” and “new” pulses are seen for several days at 327 MHz, we attribute this shift to changes in the optical path length due to interstellar refraction, in combination with timing noise. More detailed analyses of this event are presented in two companion papers (Backer et al. 2000; Lyne, Pritchard, & Graham-Smith 2000a). We find no evidence for a persistent offset in  $\nu$  or  $\dot{\nu}$  which would indicate that the rotation of the star was affected by this event.

### 3.5. Glitch 11: MJD 50812

On 1997 December 30, a rotation glitch occurred that was comparable in magnitude to Glitch 9 ( $\Delta\nu/\nu \sim 9 \times 10^{-9}$ ). The decay timescale of the transient, 2.9 d, is also typical of past glitches. Phase and frequency residuals for this glitch are shown in Figure 8, relative to a spindown model fit to 300 days before the glitch (but omitting the period around the October DM jump). The residuals have been corrected for the lingering effects of the DM jump as described by Fig. 7. However, as a comparison between Models 11a and 11b given in Table 2 indicates, even the large DM corrections inferred over this period have little effect on the glitch model, since the DM is not changing rapidly over the course of the glitch.

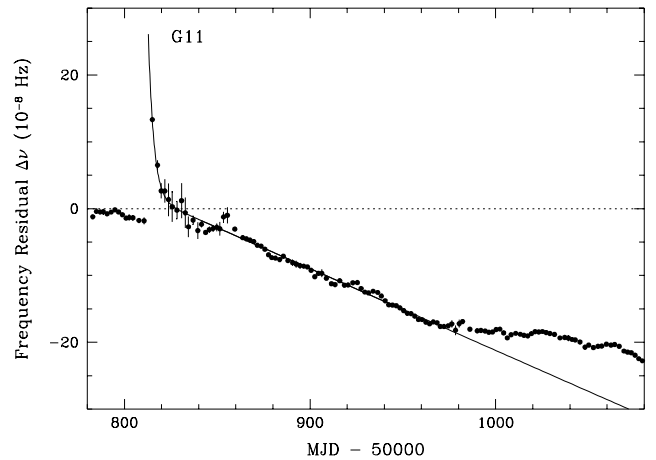


FIG. 8.— Frequency residuals showing the effects of the small glitch of 1997 December (G11) after applying the DM correction given in Figure 7. The fitted glitch model is shown as the solid line.

The most striking aspects of the postglitch recovery are a secondary spinup about 40 days after the glitch (see §4.2) and a change in  $\dot{\nu}$  about 150 days after the glitch, such that the frequency begins to deviate from the extrapolated  $\dot{\nu}$  of the glitch model (denoted by the solid line in Fig. 8). As Fig. 8 indicates, the subsequent value of  $\dot{\nu}$  is close to the preglitch value. The possibility that  $\Delta\dot{\nu}_p$  at a glitch may not be truly persistent had been tentatively raised for Glitch 7, but is even more compelling in this case. This shift in  $\dot{\nu}$  is followed by a period of particularly strong fluctuations in rotation frequency, as can be seen in Fig. 2. We attribute these fluctuations to an increase in timing noise, which may be linked to the high rate of glitching the pulsar has experienced since 1995.

### 3.6. Glitch 12: MJD 51452

Around MJD 51452 (1999 October 1), yet another glitch occurred of approximately the same magnitude as the previous one ( $\Delta\nu_0/\nu \sim 10^{-8}$ ) and with a comparable decay timescale (3.4 d). We do not yet have enough data to study the long-term effects of the glitch, although it does appear to be accompanied by a change in  $\dot{\nu}$  as was seen in the previous glitches. The best-fit parameters to the 90 days following the glitch are shown in Table 2, but more observations will be needed to obtain reliable values of  $\Delta\nu_p$

and  $\Delta\dot{\nu}_p$ . The preglitch model was fit to 450 days before the glitch.

#### 4. THE FREQUENCY OF CRAB GLITCHES

In this section we examine the occurrence in time of glitches and glitch-related events. Three idealized models are considered: (1) glitches are spaced evenly in time; (2) glitches are independent events spaced randomly in time; and (3) the glitch amplitude is proportional to the time since the last glitch. Although the statistics are hampered by the small number of glitches that have occurred during continuous observations, inclusion of the recent events appears to favor the second model (random occurrence). Finally, we present tentative evidence that some glitches may be followed by secondary spinups or “aftershocks.”

##### 4.1. Intervals between glitches

In order to study the intervals between glitches it is essential that continuous timing measurements be available. While very large glitches in the Crab are expected to leave persistent changes in  $\dot{\nu}$  that could be detectable at a later date, it is unlikely that the smaller events discussed in this paper could be inferred from data taken months or years afterward. Hence we restrict our discussion to glitches since 1982, for which continuous timing measurements from JB are available. To determine an appropriate completeness threshold, we examined a continuous 15-year frequency record (1983–1997) from JB, based on 3-day averages. We found that frequency jumps larger than  $\Delta\nu = 5 \times 10^{-8}$  Hz are clearly identifiable as either glitches or noise spikes in the data. Thus all of the glitches observed since 1986, with the exception of Glitch 10 (which we exclude from this analysis), should have been detected at any time during this interval. This yields a total sample of eight glitches and seven interglitch intervals. Although there is some question about whether Glitch 7 would have been clearly identified prior to 1995, the results presented here are qualitatively the same whether it is included or not.

The observed distribution of interglitch intervals between 1983 and 2000 is plotted cumulatively as  $S_N(T)$  in Figure 9(a), where  $S_N(T)$  is the fraction of glitches which have preceding intervals  $< T$ . The dashed curve represents the expected distribution for a Poisson process with mean interval  $\lambda$ ,

$$P(T) = 1 - e^{-T/\lambda},$$

where  $\lambda$  is taken as the mean interglitch interval (684 d). Despite the small-number statistics, the model distribution appears to be a fair match to the observations, especially if one considers only glitches since 1995, which account for all of the shorter intervals [Fig. 9(b)]. A Kolmogorov-Smirnov (K-S) test indicates that we can only reject the null hypothesis (that the observations are drawn from a Poisson model distribution) with a probability of  $\sim 30\%$ . Since the agreement with a Poisson model depends crucially on the more recent data, continued monitoring of the pulsar’s rotation will be needed to determine whether future glitches continue to follow this distribution.

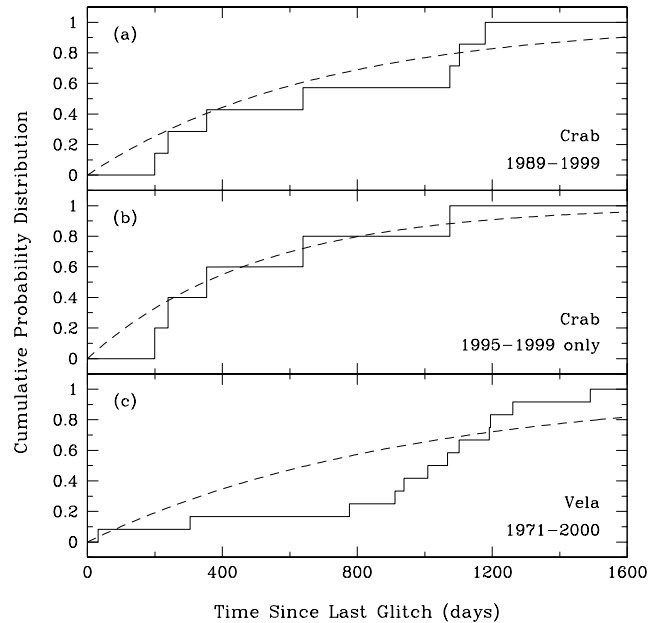


FIG. 9.— Cumulative distribution of interglitch intervals for (a) Crab glitches, intervals ending in 1989 or later; (b) Crab glitches, intervals ending in 1995 or later; (c) large Vela glitches, intervals ending in 1971 or later. The dashed curves represent models of a Poisson process having a mean interval given by the average of the intervals in each plot.

If, on the other hand, glitches tended to be spaced evenly in time, one would expect to see a steep rise in  $S_N(T)$  around the characteristic interglitch interval. Such a signature is lacking in the Crab but is present in the Vela pulsar, for which there is a tendency for glitches to be separated by  $\sim 1000$  d [Fig. 9(c)]. Here we have included only the thirteen large ( $\Delta\nu/\nu > 10^{-7}$ ) Vela glitches from 1969–2000; although two much smaller events ( $\Delta\nu/\nu \sim 10^{-8}$ ) have been reported by Cordes, Downs, & Krause-Polstorff (1988) and Flanagan (1995), they are omitted since it is unclear whether such events would have been detected over the entire 31-year timespan. Parameters for the most recent glitches (in 1996 and 2000) are taken from GB timing observations of Vela that are concurrent with the Crab observations. Although Vela shows a total range of interglitch intervals that is similar to the Crab, the shape of the distribution is substantially different, and a K-S test rules out the Poisson model (with  $\lambda=940$  d) at a 96% confidence level. Large glitches of PSR J1341–6220 may be even more regular, with four interglitch intervals of  $675 \pm 50$  d (Wang et al. 2000). The relatively constant intervals between Vela glitches have been attributed to a critical lag between the rotation of the superfluid and crust that must be achieved in order for a glitch to occur (Alpar et al. 1993).

In the third of our idealized models, the size of a glitch would be proportional to the time since the last glitch, for example if glitches empty an angular momentum reservoir that builds up between glitches at a roughly constant rate. Figure 10 shows that this is generally *not* the case for the Crab: glitches which are separated by  $\sim 1000$  d from the previous glitch still vary in amplitude by over a factor of 20. (Here the glitch amplitude is defined as  $\Delta\nu_g \equiv \Delta\nu_0 + |\Delta\nu_3|$ , i.e. any short-term rise is assumed to be unresolved.) For the large Vela glitches (solid circles), there is also no significant correlation, although including



the two small events (squares) does lead to a clear preference for small glitches to follow shortly after large ones. Nonetheless, the scatter in the relation is large, and the possibility that other small Vela glitches may have been missed needs to be evaluated. Wang et al. (2000) find that most pulsars exhibit no clear relation between glitch size and preceding interglitch interval, and conclude that the triggering of glitches is not strongly tied to the global spindown of the star.

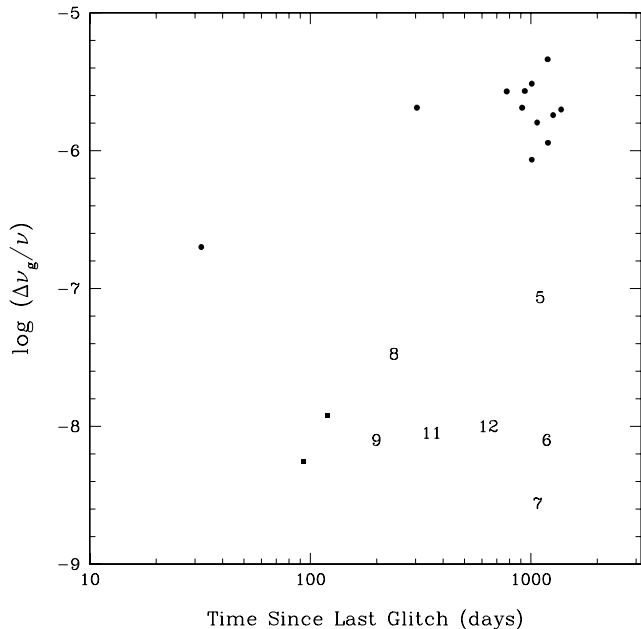


FIG. 10.— Glitch amplitude  $\Delta\nu_g/\nu$  plotted against the time since the previous glitch. Numbers indicate Crab glitches since 1989 (earlier glitches have been omitted due to possible gaps in the timing record). Filled circles indicate major Vela glitches; the two filled squares are the small Vela glitches that were omitted from Figure 9. Since they occur soon after large glitches, their inclusion in the glitch sample leads to only a minor change in the other intervals.

#### 4.2. Possible Glitch Aftershocks

Several of the small glitches observed since 1995 show indications of secondary spinups occurring  $\sim 20$ – $40$  days after the main glitch. These spinups can be identified as the first significant departures from the smooth exponential decay of the main transient, and generally show gradual rise times of  $\sim 1$  day. The most clear-cut example follows the 9th glitch, where it is classified as Glitch 10, but other smaller events (at the  $\Delta\nu \sim 10^{-8}$  Hz level) are seen following Glitches 7 and 11 (Figure 11). These latter events are comparable in magnitude to the timing noise seen between glitches, and hence their association with the glitch events is admittedly speculative. However, their morphological resemblance to Glitch 10—and the uniqueness of Glitch 10 among well-observed Crab glitches—suggest that they indeed constitute a separate class of frequency events. The deviations from a simple exponential model that were seen by Lyne & Pritchard (1987) in the residuals following Glitch 4 may also have been the result of an aftershock.

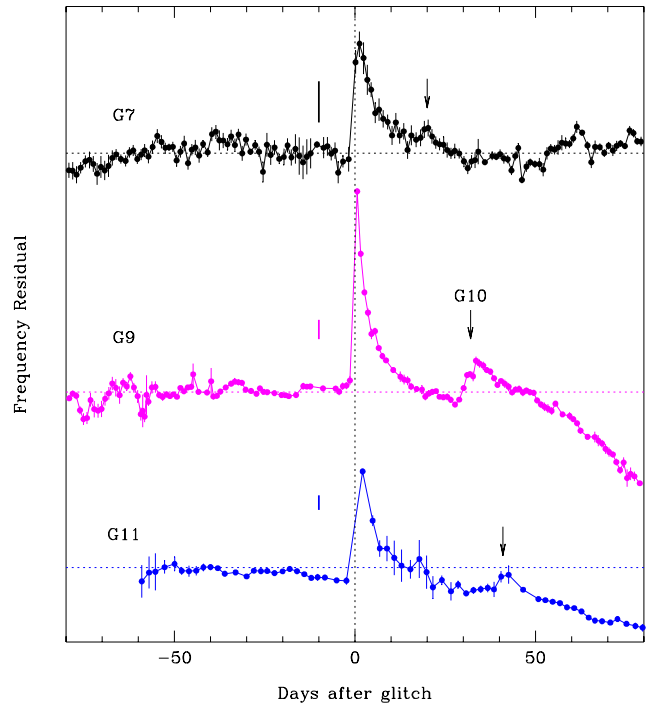


FIG. 11.— Frequency residuals for three of the small 1995–1997 glitches. Times are referenced to the assumed glitch time, which precedes the first postglitch frequency measurement by up to a few days. Arrows indicate times at which secondary spinups occur, and the vertical bar at Day  $(-10)$  corresponds to  $\Delta\nu = 2 \times 10^{-8}$  Hz.

Although further observations will be needed to confirm the association of these spinups with glitches, we suggest that future modeling of glitches include consideration of the possibility of such aftershocks, and that efforts be made to search for such features following glitches in the Crab and other pulsars. One potential difficulty is that these events are more apparent following smaller glitches, i.e. they do not appear to scale with glitch size, making it more difficult to identify them following large glitches. Thus, regular monitoring of pulsars like the Crab which display a variety of glitch sizes will be useful for exploring this issue.

## 5. OBSERVED GLITCH PROPERTIES

### 5.1. Amplitudes of the glitches

Fig. 10 displays the well-known difference in the sizes ( $\Delta\nu_g/\nu$ ) of Crab and Vela glitches. The much larger size of most Vela glitches,  $\sim 10^{-6}$ , appears to be characteristic of at least nine other pulsars as well (Lyne, Shemar, & Graham Smith 2000b; Wang et al. 2000). Still, the Crab is not unique in experiencing smaller glitches of size  $\sim 10^{-8}$ ; in fact, both Vela and PSR J1341–6220 show glitch sizes spanning a range from  $10^{-8}$ – $10^{-6}$  (Wang et al. 2000). What is noteworthy about the Crab is that it does not experience substantially larger glitches. Conventionally it has been assumed that this is due to the relative youth of the Crab pulsar; the higher crustal temperature would allow stresses due to spindown to be partially relieved by gradual processes such as plastic flow and vortex creep (e.g., McKenna & Lyne 1990; Ruderman 1991). This interpretation is consistent with the large recovery fractions seen in Crab glitches (§5.4). On the other hand, the recent observation of a large ( $\Delta\nu_g/\nu \sim 6 \times 10^{-7}$ ) glitch in

an anomalous X-ray pulsar (Kaspi, Lackey, & Chakrabarty 2000) suggests that even hot neutron stars can experience large glitches.

The same rate of angular momentum transfer from superfluid to crust can be achieved with frequent small glitches or rare large ones. Combining the sizes and frequencies of the glitches, we can define an “activity parameter”  $A_g \equiv (\sum \Delta\nu_p)/t_{obs}$ , which is the net angular momentum loss due to glitching over some observing timespan  $t_{obs}$  if persistent changes in  $\dot{\nu}$  are neglected. The advantage of  $A_g$  as a long-term indicator of glitch effects is that it is relatively insensitive to the discovery of smaller glitches as the data quality improves, unlike the analysis in §4.1 for which a threshold must be explicitly defined. The main disadvantage is that  $\Delta\nu_p$  is often not well determined for the Crab, since it depends on the glitch model employed and is generally much smaller than either the instantaneous frequency jump ( $\Delta\nu_0$ ) or the frequency change due to the change in  $\dot{\nu}$  ( $t_{obs}\Delta\dot{\nu}_p$ ).

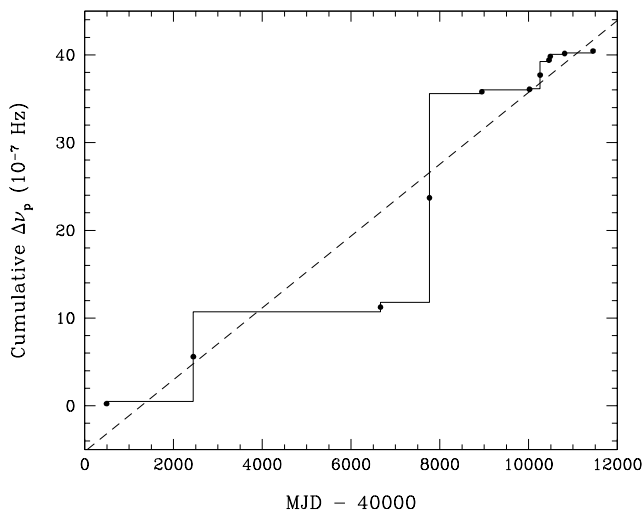


FIG. 12.— Cumulative  $\Delta\nu_p$  due to glitches plotted as a function of time based on data from Table 3. A least-squares fit to the midpoints of the frequency jumps is shown as a dashed line. The slope of this fit provides an estimate of the activity parameter  $A_g$ .

Figure 12 shows a cumulative plot of  $\Delta\nu_p$  vs. time across the historical glitch record (since 1969).  $A_g$  is given by the slope of this relation, which is  $\sim 1.3 \times 10^{-5}|\dot{\nu}|$  over the entire timespan. Excluding the recent series of glitches yields  $A_g \sim 1.1 \times 10^{-5}|\dot{\nu}|$ , an insignificant difference given the large scatter around the mean line. Thus, we see no clear evidence that the rate of angular momentum loss by the superfluid has significantly increased, despite the more frequent glitching.

### 5.2. Persistent change in $\dot{\nu}$

Our observations confirm that large Crab glitches lead to cumulative increases in  $|\dot{\nu}|$  that do not decay in time. The increase per glitch ranges from  $|\Delta\dot{\nu}/\dot{\nu}| \sim 10^{-5}$  to  $4 \times 10^{-4}$ . Alpar et al. (1996) suggest that this is a signature of the formation of new vortex “capacitors” in this young pulsar: regions that are decoupled from the regular spindown of the star and thus serve as reservoirs for storing up angular momentum. As more of the superfluid decouples, the external torque acts on a (permanently)

lower moment of inertia, increasing  $|\dot{\nu}|$ . Recent analysis of glitch behavior in a large sample of pulsars by Lyne et al. (2000b) offers indirect support for this idea. In a sample of older pulsars, the glitch activity parameter  $A_g$  (see §5.1) was roughly  $0.02|\dot{\nu}|$ , suggesting that  $\sim 2\%$  of the angular momentum outflow in pulsars is trapped in capacitive regions that only release their angular momentum in glitches. However, this percentage is considerably smaller in the Crab and a few other young pulsars, consistent with the idea that the youngest pulsars are still in the process of forming capacitors.

On the other hand, the extremely small value of  $A_g/|\dot{\nu}|$  for the Crab ( $\sim 10^{-5}$ ) is difficult to reconcile with the large values of  $\Delta\dot{\nu}/\dot{\nu} \sim 10^{-4}$  seen following glitches. The cumulative effects of the 1975, 1989, and 1996 glitches already yield  $I_{new}/I = \Delta\dot{\nu}/\dot{\nu} \sim 10^{-3}$  in 25 years, assuming no change in the external torque. Extrapolating this to the lifetime of the Crab ( $10^3$  yr) would imply that  $\sim 4\%$  of the star’s moment of inertia has already been converted into capacitors, over three orders of magnitude larger than the fraction of angular momentum released in glitches,  $A_g/|\dot{\nu}|$ . If this is in fact the case, then most of the excess angular momentum accumulating in the new capacitors cannot be released by glitching, but must continue to build over time.

Alternatively, the change in  $\dot{\nu}$  may reflect a change in the external torque, perhaps due to a change in the angle between the rotation and magnetic axes (Link, Franco, & Epstein 1998) or an increase in the dipole magnetic field (Ruderman, Zhu, & Chen 1998). If the effect is due to a change in the misalignment angle  $\alpha$ , then some mechanism must ensure that glitches only cause  $\alpha$  to increase in young pulsars such as the Crab. The inferred rate of change of  $\alpha$  is  $\sim 1.5 \times 10^{-5}$  rad yr $^{-1}$ , small enough to satisfy current observational constraints.

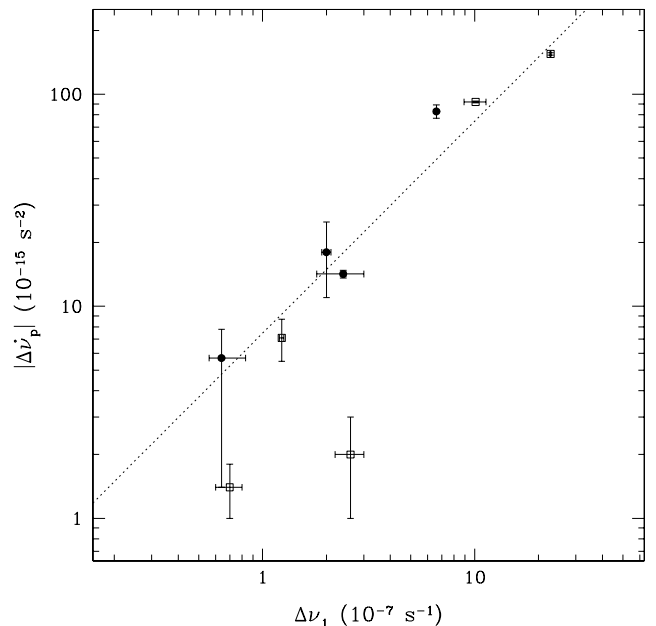


FIG. 13.— Observed correlation between the transient jump  $\Delta\nu_1$  and the persistent shift in spindown rate  $\Delta\dot{\nu}_p$ . The dotted line has a slope of  $7.5 \times 10^{-8} \text{ s}^{-1}$  or  $1/(150 \text{ d})$ . Open squares denote events before 1995 and filled circles are events presented in this paper. The most recent glitch (Glitch 12) has been omitted since its long-term recovery is not well sampled.

Although it is unclear which (if any) of these models provides the correct interpretation of the  $\Delta\dot{\nu}_p$  term, the ensemble of Crab data provides two important constraints. First of all, as shown in Figure 13, the change in  $\dot{\nu}$  at a glitch shows a good correlation with the transient jump  $\Delta\nu_1$ , with a linear correlation coefficient of 0.96 (a Spearman rank correlation gives a coefficient of 0.78). The only strongly discrepant points (at the bottom) correspond to the 1969 glitch, whose errors may well be underestimated, and the 1992 glitch. Since  $\Delta\nu_1$  dominates the frequency jump for most Crab glitches,  $\Delta\dot{\nu}_p$  also correlates well with the initial jump  $\Delta\nu_0$ ; it shows a somewhat weaker correlation with  $\Delta\nu_p$ , but displays no correlation with the time since the previous glitch (see also §4.1). These results indicate that the  $\dot{\nu}$  change is closely tied to the glitch process, and is not due to some unrelated process that is waiting for a trigger. Secondly, we have found that in Glitch 11 and possibly Glitch 7, the change in  $\dot{\nu}$  following the glitch is not truly persistent, although it does persist for much longer than the exponentially decaying term. This suggests that whatever structural changes lead to a long-term increase in  $|\dot{\nu}|$  can be partially undone at some later point, particularly when the jump in  $\dot{\nu}$  is relatively small.

### 5.3. Decay time of principal transient

The jump in frequency at a glitch is followed by a partial relaxation back towards the original frequency, which is generally interpreted as the re-establishment of an equilibrium lag between the superfluid and the crust. In this picture, there exist “resistive” regions where a continuous vortex current transfers angular momentum from the superfluid to the crust, alongside the capacitive regions where the superfluid is disconnected from the spindown of the crust. Thus, in resistive regions the crust normally feels both a *decelerative* torque from the magnetic field and an *accelerative* torque from the faster-rotating superfluid. However, when the lag is suddenly reduced in a glitch (due to excessive unpinning of vortices), the accelerative torque is also reduced and the crust spins down more rapidly ( $|\dot{\nu}|$  increases) until equilibrium is restored by vortex repinning. In the vortex creep model of Alpar et al. (1993), the recovery is exponential in time, with a timescale that reflects the ratio of the pinning energy  $E_p$  to the temperature  $kT$ .

As shown in Figure 14, the main transient component ( $\Delta\nu_1$ ), observed in 10 of the 12 glitches, has a recovery timescale that varies from about 3 to 18 days. Of the glitches since 1995, 4 have recovery times of  $\sim 3$  d and one (the largest) has a recovery time of  $\sim 10$  d. Although there is no strong correlation between the glitch amplitude and the recovery timescale, there is a slight tendency for larger glitches to have longer recovery times. One must be cautious, however, in comparing data from different timing programs, since differences in time sampling, the length of time used for the fit, or the model fitting methods employed may have significant effects on the inferred recovery timescales. For this reason we have purposely omitted the 1969 glitch, for which the exponential timescale is highly uncertain (Boynton et al. 1972). In light of these concerns, probably the strongest conclusion that can be drawn from Fig. 14 is the absence of large glitches with short recovery timescales. This is consistent with theories in which  $\tau$  increases with pinning strength (e.g. the vortex creep

model), since larger glitches would tend to result when larger pinning energies were overcome.

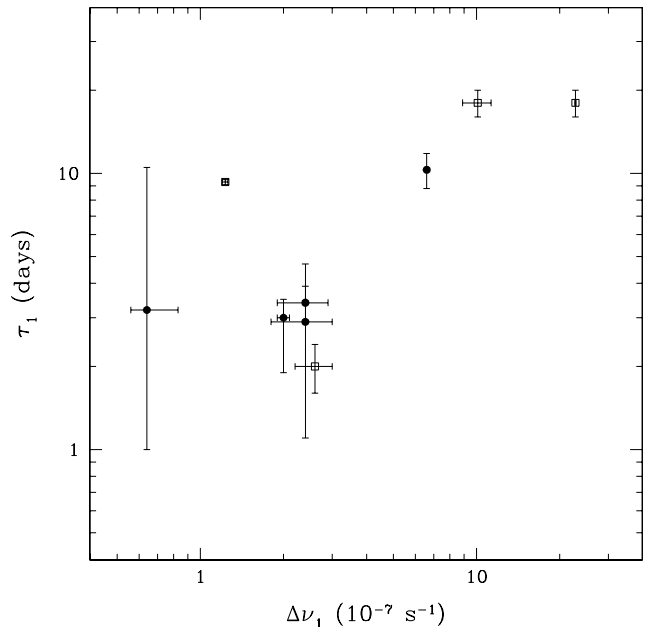


FIG. 14.— Comparison between the transient frequency jump  $\Delta\nu_1$  and its decay timescale  $\tau_1$ . Open squares denote events before 1995 and filled circles are events presented in this paper. Glitch 1 has been omitted due to poor time sampling after the glitch.

In comparison to the Crab, the recovery times following Vela glitches appear to be extremely regular. Analyzing the postglitch relaxation of the first nine glitches observed in that pulsar, Chau et al. (1993) found consistent timescales of  $3.2 \pm 0.2$  and  $33 \pm 4$  d, independent of the glitch size. (Note that these timescales are observed *simultaneously*, unlike in the Crab where a single exponential decay typically dominates each glitch.) For the 1988 and 1991 Vela glitches, an additional component of  $10 \pm 3$  hours was resolved. Fitting a glitch model to our GB data over the 100 d following the recent Vela glitch of 1996 October yields similar timescales of 3.0 and 32.0 d. Thus, our data do not appear to support the suggestion by Alpar et al. (1996) that Crab recovery timescales can be scaled by a constant factor to those seen in Vela.

### 5.4. Glitch recovery fraction

As noted in §5.2 and §5.3, the vortex creep theory of Alpar et al. (1993) postulates the existence of two types of pinning regions in the superfluid, “capacitive” regions that transfer angular momentum to the crust only in glitches, and “resistive” regions that transfer angular momentum continuously but maintain a faster equilibrium rotation than the crust. The capacitive and resistive regions give rise, respectively, to the persistent and decaying jumps in frequency that are observed at glitches. Thus, the recovery fraction

$$Q \equiv 1 - \frac{\Delta\nu_p}{\Delta\nu_0} \quad (5)$$

indicates the relative importance of resistive and capacitive regions in postglitch recovery. Lyne et al. (2000b) show that  $Q$  is a strong and monotonic function of  $\dot{\nu}$ :

young pulsars like the Crab show nearly complete recovery, while older pulsars show almost no recovery. This observation suggests that as pulsars age, resistive regions give way to capacitive ones.

An accurate test of this prediction using our data is hampered by several difficulties in assigning reliable values for  $Q$  to Crab glitches. First of all,  $Q$  is dependent on the model fit: the permanent frequency change  $\Delta\nu_p$  can only be determined once the contributions of all transient terms and the change in  $\dot{\nu}$  have been removed, and there is no guarantee that we are properly modeling these effects. Also, the initial jump  $\Delta\nu_0$  is model-dependent, derived from an extrapolation of the exponential model back to the time of the glitch. Finally, it is unclear what part of the spinup actually recovers: just the unresolved frequency jump  $\Delta\nu_0$ , or a combination of  $\Delta\nu_0$  and any short-term transient  $\Delta\nu_3$ . The fact that the main transient  $\Delta\nu_1$  exceeds  $\Delta\nu_0$  for the 1989 glitch supports the latter interpretation, which we adopt here.

In light of these uncertainties, we define for simplicity the parameter

$$\tilde{Q} \equiv \frac{\Delta\nu_1}{\Delta\nu_0 + |\Delta\nu_3|}, \quad (6)$$

which we use as a rough estimate of the recovery fraction. Values of this parameter for Crab glitches where it is well-defined are given in Table 3; it is clear that when measurable, the recovery fraction is large ( $\sim 90\%$ ). In the framework of the vortex creep model, this is consistent with the interpretation that the Crab is dominated by resistive rather than capacitive regions of vortex pinning (§5.2).

### 5.5. Time-resolved spinups

A portion of the initial spinup in Crab glitches can take much longer than the core-crust coupling timescale of  $< 1$  minute. In the 1989 glitch, part of the spinup was resolved with a 0.8 day timescale (Lyne et al. 1992), and we have noted evidence for a  $\sim 0.5$  day timescale in the 1996 glitch (§3.2). On the other hand, the Vela glitch of 1988 December exhibited a spinup that was complete in less than 2 minutes (McCulloch et al. 1990). The gradual spinups in the Crab have been linked by Alpar et al. (1996) to the formation of vortex traps: during this process, some vortex lines move in toward the rotation axis, counteracting the transfer of angular momentum to the crust and resulting in an extended spin-up. In the model of Link & Epstein (1996), on the other hand, glitches are induced by injection of heat into the inner crust (e.g., by starquakes), and the duration of the spinup is inversely related to the strength of the glitch. This is because the superfluid-lattice coupling is highly sensitive to temperature, so greater heating leads to faster and stronger glitches. Finally, Ruderman et al. (1998) suggest that resistance of magnetic flux tubes in the core to inward motion of vortex lines after the glitch may lead to a delayed spinup.

Our inability to resolve spinups in most of the smaller Crab glitches—especially the 1997 January event, for which observations commenced  $\sim 1$  hr after the glitch—argues against models in which smaller glitches occur more gradually (e.g., Link & Epstein 1996). In fact, excluding Glitch 10, which is unusual in other respects, one is led to the conclusion that only the largest glitches will have observable rise times. Such a trend is consistent with

the longer rise time seen in 1989 as compared to 1996. While the much larger yet extremely rapid spinups of the Vela pulsar do not seem to fit within this framework, age-related differences between the pulsars (e.g., in the internal temperature) may play a role.

### 5.6. Long-term asymptotic rise

A long-term asymptotic rise, such as that seen after the 1989 glitch, has not been unambiguously seen in any of the more recent glitches, possibly because the exponential timescale involved exceeds the interval between glitches. Consequently, some portion of the inferred “permanent” jumps in  $\dot{\nu}$  and  $\ddot{\nu}$  may actually be due to a long-term exponential. Indirect evidence for this interpretation comes from the fact that the braking index  $n \equiv \nu\ddot{\nu}/\dot{\nu}^2$ , when measured over intervals well-separated from glitches, shows a remarkably constant value ( $2.51 \pm 0.01$ , Lyne et al. 1993), whereas the changes in  $\dot{\nu}$  given in Table 2 would lead to changes in  $n$  of 10%–15%. However, as discussed in §3, an asymptotic exponential has the wrong curvature for explaining the residuals after Glitch 8, and provides a poor fit to the residuals after Glitch 10. Future timing observations during a long “quiescent” period in glitch activity would provide better constraints on the long-term glitch recovery process.

## 6. SUMMARY AND CONCLUSIONS

We have presented new timing observations of the Crab pulsar at 610 MHz during a period of increased glitching. The occurrence of 6 rotation glitches over a period of four years, of which 4–5 were large enough to have been detected by previous monitoring efforts, marks a departure from the relatively long intervals (3–6 years) between glitches reported prior to this period. As a result, the range of interglitch intervals has widened considerably, and shows a distribution that is consistent with a random (Poisson) process. Continued monitoring of this young pulsar will be valuable in determining whether the occurrence of glitches is primarily a regular or stochastic process.

We have also fitted simple glitch models to the data to better characterize the basic properties of Crab glitches. We summarize these properties as follows:

1. No correlation is found between the glitch amplitude and the time since the previous glitch. If vortex pinning occurs at a constant rate, this implies that glitches do not lead to the complete unpinning of vortices in a certain region.
2. In agreement with previous studies (e.g., Lyne et al. 1993), we find that Crab glitches tend to be accompanied by long-lasting (in most cases permanent) changes in spindown rate  $\dot{\nu}$ . This change in  $\dot{\nu}$  is correlates well with the transient jump  $\Delta\nu_1$  or the glitch amplitude  $\Delta\nu_0$ , and was observed to vanish or fade  $\sim 50$ – $100$  days after two of the smallest glitches.
3. The glitch amplitudes span a range of over an order of magnitude, from  $\Delta\nu/\nu \sim 2 \times 10^{-9}$  to  $3 \times 10^{-8}$ . Smaller events are unlikely to be detectable in many cases due to the substantial timing noise in this pulsar.

4. The average rate of spindown due to glitches (given by the activity parameter  $A_g$ ) has not changed significantly in recent years, despite the higher rate of glitching. This is a result of the relatively small persistent frequency jumps  $\Delta\nu_p$  accompanying the recent glitches.
5. Although a strong correlation between glitch amplitude and recovery timescale is not found, there appears to be an absence of large glitches with short recovery times, consistent with the hypothesis that the recovery time increases with the vortex pinning energy.
6. The large 1996 glitch exhibits a gradual spinup similar to that observed in the giant 1989 glitch, with a slightly shorter timescale (0.5 d rather than 0.8 d). The next glitch was a factor of  $\sim 3$  smaller and completed its spinup in under 1 hour, contradicting the hypothesis that smaller glitches have more gradual spinups (Link & Epstein 1996).
7. Detailed observations of the postglitch recovery suggest secondary spinups or “aftershocks” may follow 20–40 d after each glitch, although these events cannot clearly be distinguished from timing noise except in the case of Glitch 10 (1997 February).
8. Two of the recent glitches (1996 June and 1997 February) are accompanied by substantial changes in the frequency second derivative  $\ddot{\nu}$ , which would imply a change in the braking index  $n$  by 10–20% from its fiducial value of 2.51. A more likely explanation is that these are due to long-term transients associated with the glitches, as was seen following the 1989 event, that were interrupted by further glitches.

Our observations confirm that important differences exist between glitches in the Crab and Vela pulsars, as has been noted by other recent studies of pulsar glitches (Lyne et al. 2000b; Wang et al. 2000). Vela glitches occur at more or less regular intervals of 2–3 years, and nearly all possess similar amplitudes and recovery timescales. A spinup in Vela has never been resolved in time and the recovery fraction is fairly small ( $\sim 20\%$ , Lyne, Pritchard, & Shemar 1995). All of these properties are at odds with what has been observed in the Crab. Furthermore, most Crab glitches display persistent increases in  $|\dot{\nu}|$ , and no Crab glitches have been observed with sizes  $\Delta\nu_g/\nu \sim 10^{-6}$ , whereas such “giant” glitches have been seen in at least five young pulsars with characteristic ages  $\tau_c \equiv \nu/(2|\dot{\nu}|) = 7\text{--}16$  kyr (Wang et al. 2000), including Vela. If these differences in glitch behavior are primarily a result of evolution, they imply substantial structural changes occurring within neutron stars over their first 10 kyr.

We thank R. S. Pritchard for help in compiling the Jodrell Bank timing data. We are grateful to the NRAO staff for maintenance of the 85ft Pulsar Monitoring Telescope at Green Bank and for assistance with our observational program. Maintenance and operations of the telescope have also been supported through Naval Research Laboratory and U.S. Naval Observatory activities with the Green Bank 85ft telescopes. We thank D. Nice for his early contributions to the Green Bank effort, A. Melatos for stimulating discussions about glitch models, and A. Somer for comments on an earlier draft of this paper. Helpful comments from the referee helped to improve the paper substantially. Pulsar research at Berkeley has been supported by the University of California and NSF grants AST-9307913 in the past and currently AST-9820662. Pulsar research at Jodrell Bank is supported by a grant from the UK Particle Physics and Astronomy Research Council.

## REFERENCES

- Alpar, M. A., Chau, H. F., Cheng, K. S., & Pines, D. 1993, *ApJ*, 409, 345  
— 1996, *ApJ*, 459, 706  
Alpar, M. A., Langer, S. A., & Sauls, J. A. 1984, *ApJ*, 282, 533  
Anderson, P. W. & Itoh, N. 1975, *Nature*, 256, 25  
Backer, D. C., Wong, T., & Valanju, J. 2000, *ApJ*, in press (astro-ph/0006220)  
Boynton, P. E., Groth, E. J., Hutchinson, D. P., Nanos, G. P., Partridge, R. B., & Wilkinson, D. T. 1972, *ApJ*, 175, 217  
Chau, H. F., McCulloch, P. M., Nandkumar, R., & Pines, D. 1993, *ApJ*, 413, L113  
Cordes, J. M. 1980, *ApJ*, 237, 216  
Cordes, J. M., Downs, G. S., & Krause-Polstorff, J. 1988, *ApJ*, 330, 847  
Cordes, J. M. & Helfand, D. J. 1980, *ApJ*, 239, 640  
Demiański, M. & Prószyński, M. 1983, *MNRAS*, 202, 437  
Flanagan, C. S. 1995, *ApSS*, 230, 359  
Groth, E. J. 1975, *ApJS*, 29, 453  
Gullahorn, G. E., Isaacman, R., Rankin, J. M., & Payne, R. R. 1977, *AJ*, 82, 309  
Jones, P. B. 1998, *MNRAS*, 296, 217  
Kaspi, V. M., Lackey, J. R., & Chakrabarty, D. 2000, *ApJL*, in press  
Komesaroff, M. M., Hamilton, P. A., & Ables, J. G. 1972, *Aust. J. Phys.*, 25, 759  
Link, B. & Epstein, R. I. 1996, *ApJ*, 457, 844  
Link, B., Epstein, R. I., & Baym, G. 1992, *ApJ*, 390, L21  
Link, B., Epstein, R. I., & Lattimer, J. M. 1999, *Phys. Rev. Lett.*, 83, 3362  
Link, B., Franco, L. M., & Epstein, R. I. 1998, *ApJ*, 508, 838  
Lohsen, E. 1972, *Nat. Phys. Sci.*, 236, 70  
Lyne, A. G. & Pritchard, R. S. 1987, *MNRAS*, 229, 223  
Lyne, A. G., Pritchard, R. S., & Graham-Smith, F. 2000a, *MNRAS*, in press  
Lyne, A. G., Pritchard, R. S., & Shemar, S. L. 1995, *J. Astrophys. Astr.*, 16, 179  
Lyne, A. G., Pritchard, R. S., & Smith, F. G. 1993, *MNRAS*, 265, 1003  
Lyne, A. G., Shemar, S. L., & Graham Smith, F. 2000b, *MNRAS*, 315, 534  
Lyne, A. G., Smith, F. G., & Pritchard, R. S. 1992, *Nature*, 359, 706  
McCulloch, P. M., Hamilton, P. A., McConnell, D., & King, E. A. 1990, *Nature*, 346, 822  
McKenna, J. & Lyne, A. G. 1990, *Nature*, 343, 349  
Mendell, G. 1998, *MNRAS*, 296, 903  
Ruderman, M., Zhu, T., & Chen, K. 1998, *ApJ*, 492, 267  
Ruderman, M. A. 1991, *ApJ*, 382, 587  
Shemar, S. L. & Lyne, A. G. 1996, *MNRAS*, 282, 677  
Taylor, J. H. & Weisberg, J. M. 1989, *ApJ*, 345, 434  
Wang, N., Manchester, R. N., Pace, R. T., Bailes, M., Kaspi, V. M., Stappers, B. W., & Lyne, A. G. 2000, *MNRAS*, in press

TABLE 1  
CRAB TIMING PARAMETERS PRIOR TO 1996 GLITCH.

Parameter	Value
Right Ascension (J2000)	05 <sup>h</sup> 34 <sup>m</sup> 31 <sup>s</sup> .973
Declination (J2000)	+22°00′52″.07
Timespan for fit (MJD)	49759–50259
$\nu$ (s <sup>-1</sup> )	29.887774244
$\dot{\nu}$ (s <sup>-2</sup> )	$-3.7569761305 \times 10^{-10}$
$\ddot{\nu}$ (s <sup>-3</sup> )	$1.1857849321 \times 10^{-20}$
Braking index $n=\ddot{\nu}\nu/\dot{\nu}^2$	2.51

Note. — Astrometric coordinates are taken from Lyne, Pritchard, & Smith 1993.

TABLE 2  
MODEL FITS TO THE 1995–1999 CRAB GLITCHES.

Model	$t_g$ (MJD)	$n$	$\Delta\nu_n$ (10 <sup>-7</sup> Hz)	$\tau_n$ (days)	$\Delta\nu_p$ (10 <sup>-7</sup> Hz)	$\Delta\dot{\nu}_p$ (10 <sup>-15</sup> s <sup>-2</sup> )	$\Delta\ddot{\nu}_p$ (10 <sup>-21</sup> s <sup>-3</sup> )	$\bar{\chi}^2(\phi'_m)$	$\bar{\chi}^2(\nu'_m)$	Comments
7a*	50020.6	1	0.64	3.2	0.15	-5.7	...	7.4	2.5	Fit to 50020–50070
7b	50020.6	1	0.67	6.3	...	...	...	66.	6.4	Transient only
8a	50260.07	1	6.5	10.4	3.12	-82.9	0.85	831.	5.0	Fit to 50260–50450
8b	50260.07	1	6.4	10.2	1.23	-66.7	...	911.	5.0	No $\Delta\dot{\nu}_p$ term, slow expon. decay
8c*	50259.93	1	6.6	10.3	3.14	-83.0	0.86	833.	4.5	Short-term rise
		3	-3.1	0.5						
9*	50459.15	1	2.01	3.0	0.32	-18.2	...	8.8	2.8	Fit to 50459–50487
10a	50489	...	...	...	0.47	-4.4	-2.15	2215.	11.7	Fit to 50491–50811
10b*	50489	3	-0.33	2.2	0.50	-4.8	-2.13	3004.	8.9	Incl. JB 50486-91
10c	50489	2	-33.3	381.	33.7	-101.4	...	10927.	21.9	Asymptotic expon.
11a	50812.9	1	2.46	2.5	0.22	-14.5	...	36.9	5.7	Fit to 50812–50950
11b*	50812.9	1	2.44	2.9	0.17	-14.2	...	38.1	4.9	DM-corrected
12*	51452.3	1	2.43	3.4	0.44	-6.0	...	770.	39.1	Fit to 51453–51543

Note. — Each transient component is classified as a short to intermediate term decay ( $n=1$ ), a long-term rise or decay ( $n=2$ ), or a short-term asymptotic rise ( $n=3$ ). Asterisks (\*) denote adopted fits.

TABLE 3  
ADOPTED PARAMETERS FOR ALL OBSERVED CRAB GLITCHES.

No.	UT Date	$t_g$ (MJD)	$\Delta\nu_0$ ( $10^{-7}$ Hz)	$n$	$\Delta\nu_n$ ( $10^{-7}$ Hz)	$\tau_n$ (days)	$\Delta\nu_p$ ( $10^{-7}$ Hz)	$\Delta\dot{\nu}_p$ ( $10^{-15}$ s $^{-2}$ )	$\Delta\ddot{\nu}_p$ ( $10^{-21}$ s $^{-3}$ )	$\tilde{Q}$
1	69-09-30	40494	$1.2 \pm .1$	1	$0.7 \pm .1$	$18.7 \pm 1.6$	$0.5 \pm .1$	$-1.4 \pm .4$	...	0.58
2	75-02-04	42447.5	$13.2 \pm .2$	1	$10.1 \pm 1.2$	$18 \pm 2$	$10.2 \pm 1.2$	$-92 \pm 1$	...	0.77
				2	$-7.07 \pm 0.1$	$97 \pm 4$				
3	81-??-??	$\sim 44900$	...	2	$-2.8 \pm .1$	$222 \pm 20$	2.8?	$-3.8 \pm .7$	...	...
4	86-08-22	46664.4	$1.23 \pm .03$	1	$1.23 \pm .03$	$9.3 \pm .2$	$1.1 \pm .1$	$-7.1 \pm 1.6$	...	1.00
				2	$-1.1 \pm .1$	$123 \pm 40$				
5	89-08-29	47767.4	$\sim 18.5$	1	$22.8 \pm .1$	$18 \pm 2$	$23.8 \pm .2$	$-155 \pm 2$	...	0.89
				2	$-21.1 \pm .1$	$265 \pm 5$				
				3	$-7$	$0.8$				
6	92-11-21	$48947.0 \pm .2$	$3.0 \pm .4$	1	$2.6 \pm .4$	$2.0 \pm .4$	$0.4 \pm .1$	$-2 \pm 1$	...	0.87
7	95-10-30	$50020.6 \pm .3$	$0.8 \pm .2$	1	$0.64^{+.19}_{-.08}$	$3.2^{+7.3}_{-2.2}$	$0.15^{+.05}_{-.15}$	$-5.7^{+4.3}_{-2.1}$	...	0.80
8	96-06-25	$50259.93^{+.25}_{-.01}$	$\sim 6.6$	1	$6.6 \pm .1$	$10.3 \pm 1.5$	$3.1 \pm .3$	$-83 \pm 6$	$0.9 \pm .6$	0.68
				3	$-3.1$	$0.5$				
9	97-01-11	$50459.15 \pm .05$	$2.3 \pm .1$	1	$2.0 \pm .1$	$3.0^{+0.5}_{-1.1}$	$0.32 \pm .13$	$-18 \pm 7$	...	0.87
10	97-02-10	$50489.0^{+2.5}_{-0.5}$	$\sim 0.2$	3	$-0.3$	$2.2$	$0.50 \pm .08$	$-4.8 \pm 1.8$	$-2.1 \pm .7$	...
11	97-12-30	$50812.9^{+0.3}_{-1.5}$	$2.6 \pm .7$	1	$2.4 \pm .6$	$2.9 \pm 1.8$	$0.17 \pm .05$	$-14.2 \pm .6$	...	0.92
12	99-10-01	$51452.3^{+1.2}_{-1.6}$	$2.9 \pm .5$	1	$2.4 \pm .5$	$3.4 \pm .5$	$0.4 \pm .1$	$-6 \pm 2$	...	0.83

Note. — Data from the first five glitches are taken from Lyne, Pritchard, & Smith 1993.